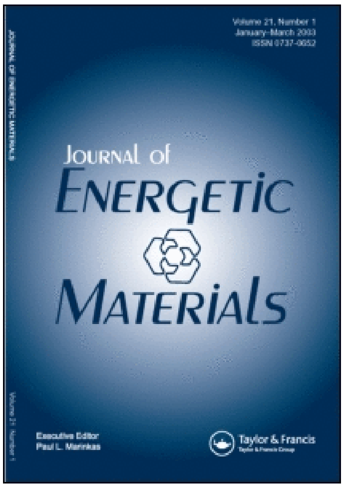

Journal of Energetic Materials
Publication details, including instructions for authors and subscription information:
http://www.informaworld.com/smpp/title~content=t713770432

The V_1V_2 EOS for Detonation Products

Yehuda Partom

To cite this Article Partom, Yehuda(2010) 'The V_1V_2 EOS for Detonation Products', Journal of Energetic Materials, 28: 1, 263 — 278
To link to this Article: DOI: 10.1080/07370651003781652
URL: http://dx.doi.org/10.1080/07370651003781652

Journal of Energetic Materials, 28: 263–278, 2010
Copyright © Taylor & Francis Group, LLC
ISSN: 0737-0652 print/1545-8822 online
DOI: 10.1080/07370651003781652

The V_1V_2 EOS for Detonation Products

YEHUDA PARTOM

Rafael, Haifa, Israel

Many equations of state (EOS) for detonation products have been proposed and used. Some of them are in analytical form and some in tabular form. The most popular is the Jones-Wilkins-Lee (JWL) EOS. One of the main parameters of a product's EOS is the so-called adiabatic gamma along its main isentrope (γ_s). For JWL EOSs $\gamma_s(V)$ varies in a nonmonotonic way. Going down from the CJ point along the main isentrope, it first increases to create a hump, and then, as V goes to infinity, gamma decreases to perfect gas-like behavior with gamma around 1.3. But according to Davis [1], $\gamma_s(V)$ should decrease monotonically with V. Accordingly, in this article we investigate the following: (1) Is the hump in $\gamma_s(V)$ necessary? and (2) Is it possible to construct a product's EOS with a monotonic $\gamma_s(V)$ that is consistent with experimental data? We find that (1) it is possible to construct a product's EOS without a hump in $\gamma_s(V)$; and (2) without a hump in $\gamma_s(V)$ there are not enough degrees of freedom to reproduce cylinder test data.

Keywords: detonation, detonation products, equation of state, modeling

Introduction

Many equations of state (EOSs) for detonation products have been proposed and used. Some of them are in analytical form and some in tabular form. The most popular is the

Address correspondence to Yehuda Partom, Rafael, P.O. Box 2250, Haifa 31021, Israel. E-mail: ypartom@netvision.net.il

Jones-Wilkins-Lee (JWL) EOS. The main isentrope (the isentrope through the Chapman-Jouguet [CJ] point) of the JWL EOS includes six adjustable parameters. These are adjusted to fulfill the four following conditions:

- The three Hugoniot jump conditions, assuming that the CJ detonation velocity is known from tests.
- The CJ (sonic) condition (the Raleigh line is tangent to the Hugoniot and to the isentrope at the CJ point).

Because the number of adjustable parameters is larger than the number of conditions, the remaining conditions are fulfilled from tests, usually expanding cylinder tests (ECT).

The JWL EOS is a Gruneisen EOS referring to the main isentrope with a constant Gruneisen gamma (Γ).The standard choice is $\Gamma = \mathrm{w}$, where w is one of the main isentrope parameters.

The adiabatic gamma along the main isentrope $\mathrm{P_s(V)}$ is defined as:

$$\gamma_\mathrm{s} = -\frac{\mathrm{V}}{\mathrm{P_s}}\frac{\mathrm{dP_s}}{\mathrm{dV}} = -\frac{\mathrm{d}\,\ell\mathrm{nP_s}}{\mathrm{d}\,\ell\mathrm{nV}} \tag{1}$$

Evaluating $\gamma_\mathrm{s}(\mathrm{V})$ with JWL for a common explosive, we get the curve shown in Fig. 1. We see from Fig. 1 that $\gamma_\mathrm{s}(\mathrm{V})$ has a positive slope at the CJ point. As V increases, it increases to a quite high maximum (hump) and then decreases to $1 + \mathrm{w}$ as V goes to infinity. For some common explosives $\gamma_\mathrm{s}(\mathrm{V})$ has even two humps.

Bill Davis [1] outlined schematically the expected variation of the functions $\gamma_\mathrm{s}(\mathrm{V})$ and $\Gamma(\mathrm{V})$. In Fig. 2 we reproduce his schematic curves. We see from Fig. 2 that both curves are monotonically decreasing and have no humps. Bill Davis [1] did not provide a justification for his schematic curves. Eight years later, Bill Davis [2] showed similar curves, but that time they were not schematic, and $\gamma_\mathrm{s}(\mathrm{V})$ did have a hump. We reproduce these curves in Fig. 3.

With this background we ask the following questions:

- Is it possible to construct a main isentrope for the product's EOS that will have a monotonically decreasing $\gamma_\mathrm{s}(\mathrm{V})$ curve as in Fig. 2?

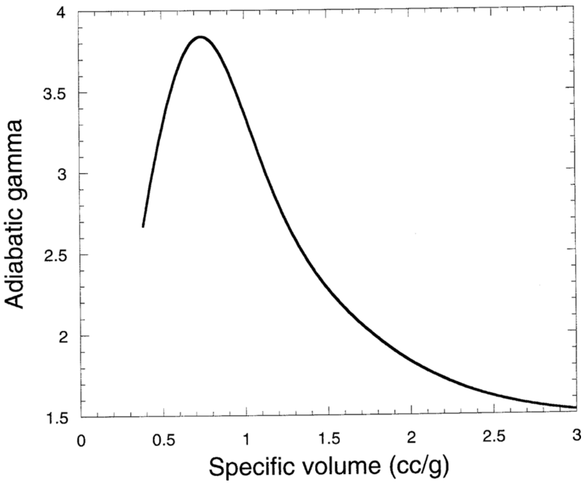

Figure 1. Adiabatic gamma as a function of specific volume, $\gamma_s(V)$, for a common explosive using the standard JWL parameters.

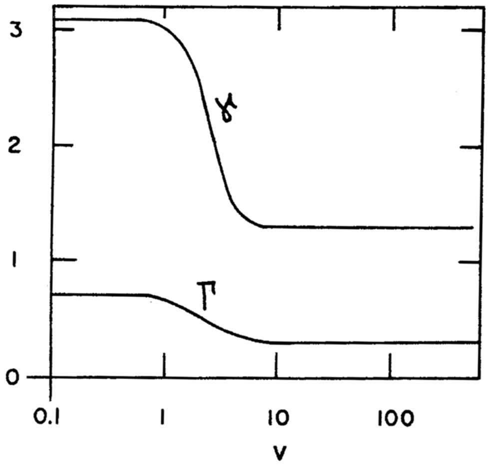

Figure 2. Adiabatic gamma and Gruneisen gamma as a function of specific volume, according to Davis [1].

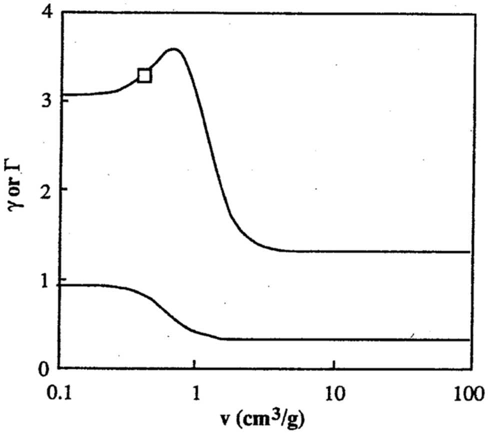

Figure 3. Adiabatic gamma and Gruneisen gamma as a function of specific volume, according to Davis [2].

- For such a main isentrope, is it possible for the EOS that refers to it to reproduce ECT data?

The standard approach to model the main isentrope has been (1) assume a $P_s(V)$ relation with enough adjustable parameters; (2) adjust the parameters to satisfy CJ conditions and metal expansion data. Examples of this approach are given in the literature [2–8]. The JWL main isentrope, developed with this approach, has a hump and sometimes two humps to the right of V_{CJ}, as seen in Fig. 1 and in Kury et al. [5] and Lee et al. [7]. A qualitative explanation of the first hump is given in Lee et al. [7], but there were others who called the humps (or at least the second one) nonphysical.

What triggered this work is Davis's claim [1] that $\gamma_s(V)$ has to be monotonically decreasing. Our approach is different from the standard approach in that it assumes $\gamma_s(V)$ explicitly (instead of assuming $P_s(V)$). In this way we are able to find out whether a hump is really necessary and for what reasons. We do this by running a hydro-code with the cylinder test and a trial $\gamma_s(V)$ and seeing the consequences in the $u(r - r_0)$ curve.

Recently we developed this approach further. We assume $\gamma_s(V)$ as a piecewise linear function in the range of interest. This enables us to adjust the discrete values $\gamma_s(V_i)$ recursively, from left to right, and there is no need to solve a complex system of equations. We plan to include this work in a subsequent paper.

The V_1V_2 EOS

We first write down equations for a monotonically decreasing main isentrope. For simplicity, we omit the index s from the functions $\gamma_s(V)$, $P_s(V)$, and $E_s(V)$ along it. For $\gamma(V)$ we assume a monotonically decreasing curve (as in Fig. 2), composed of three straight lines. We show this $\gamma(V)$ in Fig. 4. To evaluate P(V) and E(V) along this isentrope we integrate Eq. (1) and then the energy Eq. (2).

$$\frac{dE}{dV} = -P \tag{2}$$

For the section $V \geq V_2$ we get:

$$\begin{aligned} P &= P_2\left(\frac{V}{V_2}\right)^{-\gamma_\infty} \\ E &= E_2\left(\frac{V}{V_2}\right)^{-\gamma_\infty+1}; \quad E_2 = \frac{P_2V_2}{\gamma_\infty - 1} \end{aligned} \tag{3}$$

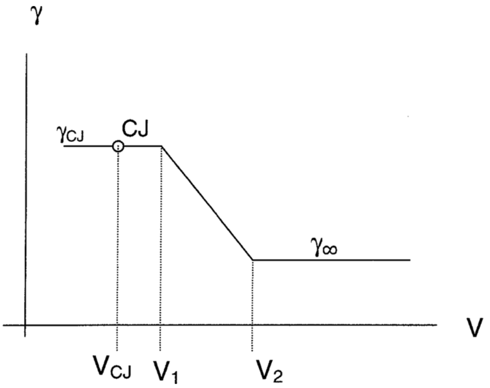

Figure 4. Schematic description of $\gamma_s(V)$ for the V_1V_2 EOS.

For $V \leq V_1$ we get:

$$P = P_{CJ}\left(\frac{V}{V_{CJ}}\right)^{-\gamma_{CJ}}; \quad P_1 = P_{CJ}\left(\frac{V_1}{V_{CJ}}\right)^{-\gamma_{CJ}} \tag{4}$$

where V_{CJ} is given from the CJ condition by:

$$V_{CJ} = V_0\frac{\gamma_{CJ}}{\gamma_{CJ}+1} \tag{5}$$

and where P_{CJ} is given from mass and momentum conservation jump conditions by:

$$P_{CJ} = \rho_0^2 D^2(V_0 - V_{CJ}) = \frac{\rho_0 D^2}{\gamma_{CJ}+1} \tag{6}$$

where D is the CJ detonation velocity.

Also, integrating Eq. (4) we get:

$$\begin{aligned} E &= E_{CJ}\frac{P_{CJ}V_{CJ}}{\gamma_{CJ}-1}\left[\left(\frac{V}{V_{CJ}}\right)^{-\gamma_{CJ}+1} - 1\right] \\ E_1 &= E_{CJ}\frac{P_{CJ}V_{CJ}}{\gamma_{CJ}-1}\left[\left(\frac{V_1}{V_{CJ}}\right)^{-\gamma_{CJ}+1} - 1\right] \end{aligned} \tag{7}$$

where E_{CJ} and the heat of detonation Q are related by the energy jump condition:

$$E_{CJ} = \frac{1}{2}P_{CJ}(V_0 - V_{CJ}) + Q \tag{8}$$

For $V_1 \leq V \leq V_2$ we get:

$$\begin{aligned} &\gamma = a + bV \\ &a = \frac{\gamma_{CJ}V_2 - \gamma_\infty V_1}{V_2 - V_1}; \quad b = -\frac{\gamma_{CJ} - \gamma_\infty}{V_2 - V_1} \end{aligned} \tag{9}$$

$$\begin{aligned} &\gamma = \mathrm{a} + \mathrm{bV} = \frac{\mathrm{dP}}{\mathrm{dV}}\frac{\mathrm{V}}{\mathrm{P}} \\ &\therefore \mathrm{P} = \mathrm{AV}^{-\mathrm{a}}\exp(-\mathrm{bV}) \end{aligned} \tag{10}$$

Substituting V_1,P_1 from Eq. (4) into Eq. (10) we get:

$$\begin{aligned} &\mathrm{A} = \mathrm{P}_1\mathrm{V}_1^{\mathrm{a}}\exp(\mathrm{bV}_1) \\ &\mathrm{P} = \mathrm{P}_1\left(\frac{\mathrm{V}}{\mathrm{V}_1}\right)^{-\mathrm{a}}\exp[-\mathrm{b}(\mathrm{V}-\mathrm{V}_1)] \\ &\mathrm{P}_2 = \mathrm{P}_1\left(\frac{\mathrm{V}_2}{\mathrm{V}_1}\right)^{-\mathrm{a}}\exp[-\mathrm{b}(\mathrm{V}_2-\mathrm{V}_1)] \end{aligned} \tag{11}$$

To sum up, the main isentrope P(V) is given by:

$$\begin{aligned} &\mathrm{P} = \mathrm{P}_{\mathrm{CJ}}\left(\frac{\mathrm{V}}{\mathrm{C}_{\mathrm{J}}}\right)^{-\gamma_{\mathrm{CJ}}} \quad \text{for } \mathrm{V} \le \mathrm{V}_1 \\ &\mathrm{P} = \mathrm{P}_1\left(\frac{\mathrm{V}}{\mathrm{V}_1}\right)^{-\mathrm{a}}\exp[-\mathrm{b}(\mathrm{V}-\mathrm{V}_1)] \quad \text{for } \mathrm{V}_1 \le \mathrm{V} \le \mathrm{V}_2 \\ &\mathrm{P} = \mathrm{P}_2\left(\frac{\mathrm{V}}{\mathrm{V}_2}\right)^{-\gamma_\infty} \quad \text{for } \mathrm{V} \ge \mathrm{V}_2 \end{aligned} \tag{12}$$

where

$$\mathrm{P}_1 = \mathrm{P}_{\mathrm{CJ}}\left(\frac{\mathrm{V}}{\mathrm{V}_{\mathrm{CJ}}}\right)^{-\gamma_{\mathrm{CJ}}}; \quad \mathrm{P}_2 = \mathrm{P}_1\left(\frac{\mathrm{V}_2}{\mathrm{V}_1}\right)^{-\mathrm{a}}\exp[-\mathrm{b}(\mathrm{V}_2-\mathrm{V}_1)] \tag{13}$$

and where V_{CJ} is given by Eq. (5) and P_{CJ} by Eq. (6), and where the CJ detonation velocity D is known from tests.

The internal energy E(V) along the section $V_1 \le V \le V_2$ is given by the integral:

$$\mathrm{E} = \mathrm{E}_2 - \int_{\mathrm{V}_2}^{\mathrm{V}} \mathrm{P}(\mathrm{V})\,\mathrm{dV}; \ \mathrm{V}_1 \le \mathrm{V} \le \mathrm{V}_2 \tag{14}$$

where E_2 is given by Eq. (3), and P_2, appearing in Eq. (3), is given by Eq. (13).

But because P(V) along this section (given by Eq. (12)) is not analytically integrable, we evaluate the integral in Eq. (14) numerically, and during the integration process we construct a table V_i,E_i. Later, when we use the EOS in a hydro-code, we determine E in this section by linearly interpolating between neighboring points in this table.

From the numerical integration we also get the value of E_1:

$$E_1 = E_2 - \int_{V_2}^{V_1} P(V)\,dV \tag{15}$$

and substituting E_1 into the second of Eq. (7) we obtain E_{CJ}.

When the heat of detonation Q is not known, it can be determined from Eq. (8). But when Q is known, Eq. (8) is used to determine some other parameter. Usually we use Eq. (8) to determine the parameter γ_∞.

On the basis of the main isentrope described above we define a Gruneisen EOS in the usual way:

$$E = E_s(V) + \frac{V}{\Gamma(V)}[P - P_s(V)] \tag{16}$$

where in Eq. (16) we put back the index s along the main isentrope, and where we assume that $\Gamma(V)$ is varying similar to $\gamma_s(V)$, as shown schematically in Fig. 2:

$$\begin{aligned} &\Gamma = \Gamma_{CJ} \quad \text{for } V \le V_1 \\ &\Gamma = \Gamma_\infty = \gamma_\infty - 1 \quad \text{for } V \ge V_2 \\ &\Gamma = a_\Gamma + b_\Gamma V \quad \text{for } V_1 \le V \le V_2 \end{aligned} \tag{17}$$

$$a_\Gamma = \frac{\Gamma_{CJ} V_2 - \Gamma_\infty V_1}{V_2 - V_1}; \quad b_\Gamma = -\frac{\Gamma_{CJ} - \Gamma_\infty}{V_2 - V_1} \tag{18}$$

We determine Γ_{CJ} to reproduce the experimental value of the derivative of detonation velocity with respect to initial density. The equations for that (known as the Jones-Stanyukovich-Manson [JSM] equations) are

$$\begin{aligned} \mathrm{k} &= \frac{\rho_0}{\mathrm{D}}\frac{\mathrm{dD}}{\mathrm{d}\rho_0} = \frac{\mathrm{d}\,\ell\mathrm{n}(\mathrm{D})}{\mathrm{d}\,\ell\mathrm{n}(\rho_0)} \\ \alpha &= \frac{\gamma - 1 - 2\mathrm{k}}{1+\mathrm{k}}; \quad \Gamma = \frac{\alpha}{1+\alpha}\gamma \end{aligned} \tag{19}$$

where α is known as the Jones parameter, and where the quantities in Eq. (19) are at the CJ point. For the common explosive of Fig. 1 the values of these quantities are

$$\frac{\mathrm{dD}}{\mathrm{d}\rho_0} = 2.7\,\frac{\mathrm{km/s}}{\mathrm{g/cc}}; \quad \frac{\mathrm{D}}{\rho_0} = 4.07\frac{\mathrm{km/s}}{\mathrm{g/cc}}; \quad \mathrm{k} = 0.66 \tag{20}$$

and for $\gamma_{\mathrm{CJ}} = 3.25$ (a value that we use later) we get:

$$\alpha_{\mathrm{CJ}} = 0.56; \quad \Gamma_{\mathrm{CJ}} = 1.17 \tag{21}$$

In the next section we make use of this EOS in calculations of ECT.

Expanding Cylinder Test Simulations

We perform standard ECT simulations for two purposes:

- To compare simulations with the $\mathrm{V_1V_2}$ EOS to simulations with the JWL EOS and to test data.
- To check the sensitivity of the results to the values of the adjustable parameters.

The standard ECT configuration is

- The dimensions of the explosive cylinder are 25 mm diameter and 300 mm length.
- The explosive is inside a copper shell 2.5 mm thick.
- The explosive is initiated by a plane wave on one of its edges.

- The copper shell motion is monitored at a distance of 200 mm from the initiation plane.
- Diagnostics (preferably with a VISAR) include the radial velocity (u) as function of the radial displacement $(\mathrm{r}-\mathrm{r}_0)$.

We use the PISCES commercial code, and the detonation scheme is the PISCES ONTIME (like programmed burn). The mesh in the explosive is two cells per millimeter in both directions. The mesh in the copper is two cells per millimeter in the longitudinal direction and four cells per millimeter in the radial direction.

The first run is with the JWL EOS, and we compare the results of this run with test data given in Gibbs and Popolato [9]. We show the comparison in Fig. 5. We see from Fig. 5 that the simulation with the JWL EOS reproduces the test data rather decently, at least beyond a radial displacement of 5 mm. We assume that the JWL EOS would also reproduce the initial velocity steps. We regard the JWL results as representing the data, and we compare all the $\mathrm{V}_1\mathrm{V}_2$ simulations to

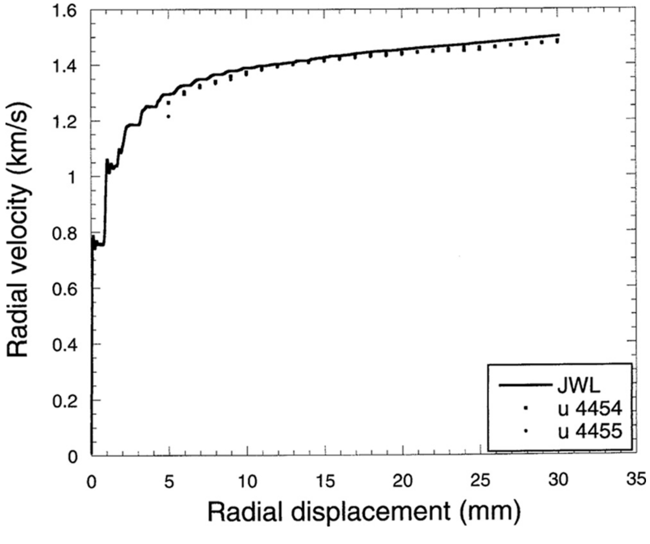

Figure 5. Radial velocity as a function of radial displacement in ECT. Comparison of JWL simulation with experimental data.

them. We regard the following parameters of the $\mathrm{V_1V_2}$ EOS as nominal:

$$\begin{aligned} &\gamma_{\mathrm{CJ}} = 3.25; \quad \mathrm{Q} = 3.73\,\mathrm{kJ/g} \\ &\mathrm{V_1} = 1\,\mathrm{cc/g}; \quad \mathrm{V_2} = 3\,\mathrm{cc/g} \end{aligned} \tag{22}$$

and γ_∞ that fits these values is $\gamma_\infty = 1.441$.

In Fig. 6 we compare the $\mathrm{u(r - r_0)}$ curve obtained with JWL to that obtained with $\mathrm{V_1V_2}$ with the nominal set of parameters. We see from Fig. 6 that after the initial steps the agreement is quite good, but the initial steps do not agree. The reason is that to get an agreement at late times we have to use a value of γ_{CJ} that is much higher than the one used with JWL. It seems that the high value we use for γ_{CJ} is some kind of average of the hump shown in Fig. 1.

In Fig. 7 we check the influence of decreasing γ_{CJ}. We see from Fig. 7 that, as expected, the levels of the initial velocity steps increase, but the late time portion of the curve also increases significantly.

In Fig. 8 we check the influence of changing the heat of detonation Q. We decrease Q from 3.73 to 3.50 kJ/g. The value of

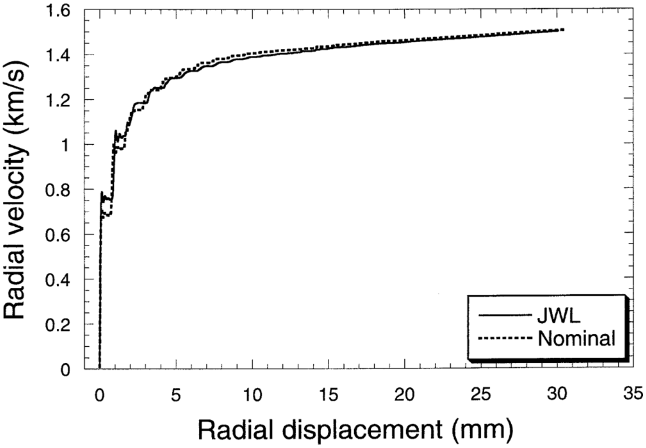

Figure 6. Radial velocity as a function of radial displacement in ECT. Comparison of $\mathrm{V_1V_2}$ with JWL.

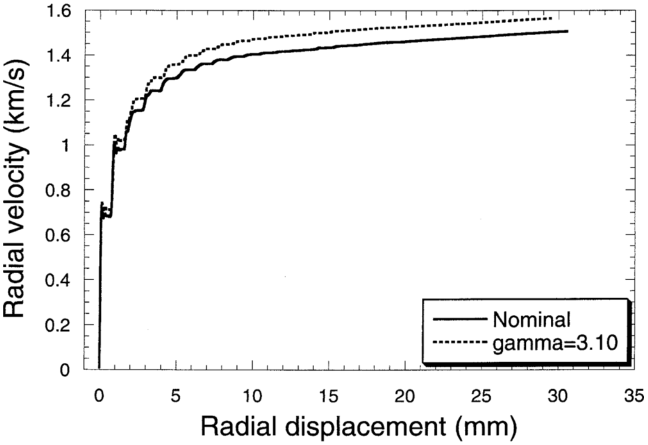

Figure 7. Radial velocity as a function of radial displacement in ECT. Sensitivity to γ_{CJ}.

γ_∞ that goes along with this is $\gamma_\infty = 1.638$. We see from Fig. 8 that the influence of Q is rather small and that it can be detected only at late times.

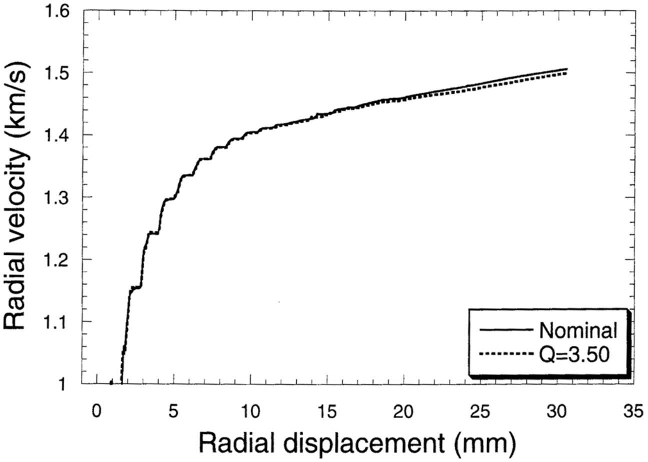

Figure 8. Radial velocity as a function of radial displacement in ECT. Sensitivity to Q.

In Fig. 9 we check the influence of the parameter V_1. We change V_1 from 1 to $2\,\mathrm{cm}^3/\mathrm{g}$. The appropriate value of γ_∞ is $\gamma_\infty = 1.255$. We see from Fig. 9 that increasing V_1 lowers the $u(r - r_0)$ curve but only at late times.

In Fig. 10 we check the influence of changing V_2 from 3 to $5\,\mathrm{cm}^3/\mathrm{g}$. The appropriate value of γ_∞ is $\gamma_\infty = 1.224$. We see from Fig. 10 that the effect of changing V_2 is also quite small and comes about at late times.

From the parameter sensitivity check we conclude that

- The largest sensitivity is to the parameter γ_{CJ}. Increasing γ_{CJ} decreases the initial velocity steps and vice versa. To get the correct levels of the initial velocity steps we need to use $\gamma_{CJ} = 3.10$, but then the level at late time is much too high, and it is not possible to lower it down to the needed value by changing the other parameters.
- The influence of the other three parameters Q, V_1, and V_2 is quite small, and it comes about only at late times.
- The V_1V_2 EOS (with monotonically decreasing γ_s) does not have enough degrees of freedom to reproduce the

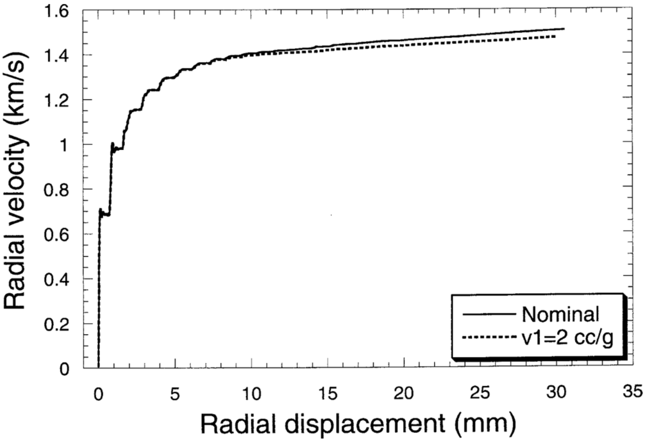

Figure 9. Radial velocity as a function of radial displacement in ECT. Sensitivity to V_1.

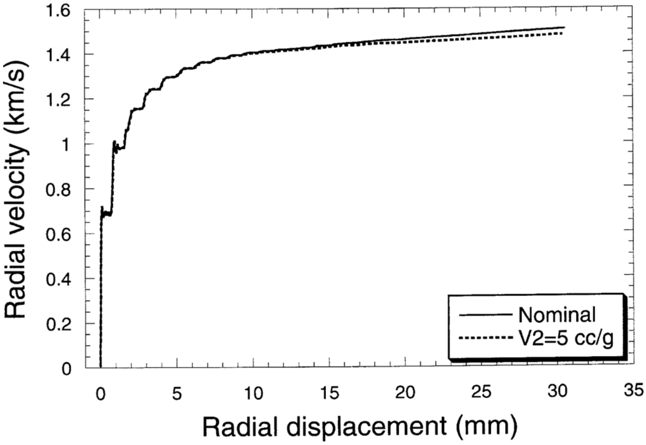

Figure 10. Radial velocity as a function of radial displacement in ECT. Sensitivity to V_2.

whole $u(r - r_0)$ curve obtained from an ECT. To be able to reproduce the experimental curve we need to add one or more degrees of freedom by introducing a hump to the right of the CJ point. In Fig. 11 we show a schematic example like that with one additional parameter (γ_1).

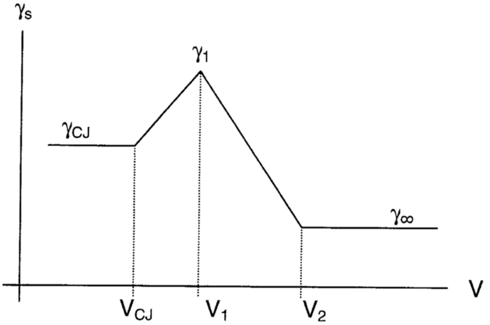

Figure 11. A schematic description of a piecewise linear $\gamma_s(V)$ curve with a hump.

Summary

Computing the adiabatic gamma (γ_s) along the main isentrope of the JWL EOS, one gets a hump to the right of the CJ point. A hump like this means that in $\log P - \log V$ space, the adiabat dips below the straight line adiabat through the CJ point, which has a slope of γ_{CJ}. Experimental evidence on this was obtained by many labs [3–5], but we are not aware that theoretical justification has been derived from basic considerations or from chemical equilibrium EOSs. We therefore check here whether it is possible to construct a product's EOS based on a main isentrope that has a monotonically decreasing $\gamma_s(V)$. We use a piecewise linear $\gamma_s(V)$ curve, and we call the EOS based on it the V_1V_2 EOS.

We apply V_1V_2 in simulations of a standard ECT. We compare to a JWL simulation (which is shown to reproduce test data), and we conduct a parameter sensitivity study. We find that

- It is possible to adjust the parameters to reproduce the JWL result beyond the initial velocity jumps.
- The parameter γ_{CJ} affects the whole curve (shell velocity versus shell displacement), including the initial velocity jumps.
- The other three parameters affect only the late time level of the velocity curve.
- To get full agreement with ECT data we need to add one or more degrees of freedom to $\gamma_s(V)$, which means to introduce a hump to the right of the CJ point.

References

[1] Davis, W. C. 1985. Equation of State for Detonation Products. In *Proceedings of the 8th Symposium for Detonation*, ed. J. Short, pp. 785–798, Albuquerque, NM.

[2] Davis, W. C. 1993. Equation of state for detonation products. In *Proceedings of the 10th Symposium for Detonation*, ed. J. Short, pp. 369–375, Boston, MA.

[3] Wilkins, M. L. 1964. The Equation of State of PBX-9404 and LX-04-01, LLNL, UCRL-7797.

[4] Wilkins, M. L. 1943. Calculation of Elastic-Plastic Flow, LLNL, UCRL-7322.

[5] Kury, J. W., H. C. Hornig, E. L. Lee, L. McDonell, D. L. Ornellas, M. Finger, F. M. Strange, and M. L. Wilkins. 1965. Metal Acceleration by Chemical Explosives. *Proceedings of the 4th Symposium on Detonation*, ed. J. Short, pp. 3–13, White Oak, MD.

[6] Allan, J. W. S. and B. D. Lambourn. 1965. An equation of state of products at pressures below 30 kilobars. *Proceedings of the 4th Symposium on Detonation*, ed. C. J. Jacobs, pp. 52–66, White Oak, MD.

[7] Lee, E. L., H. C. Hornig, and J. W. Kury. 1968. Adiabatic expansion of high explosive detonation products. LLNL Report. TID-4500, UC-4.

[8] Davis, W. C. 1993. 1998. Equation of state for detonation products. *The 11th Symposium on Detonation*, ed. J. Short, pp. 303–308, Snowmass, CO.

[9] Gibbs, T. R. and A. Popolato. 1980. *LASL Explosive Property Data*. Berkeley, CA: University of California Press.